Original Paper

phys. stat. sol. (a) **204**, No. 6, 1987–1995 (2007) / **DOI** 10.1002/pssa.200674894

Nitride intersubband devices: prospects and recent developments

F. H. Julien[*, 1], **M. Tchernycheva**[1], **L. Nevou**[1], **L. Doyennette**[1], **R. Colombelli**[1], **E. Warde**[1], **F. Guillot**[2], and **E. Monroy**[2]

[1] Institut d'Electronique Fondamentale, UMR 8622 CNRS, Universite Paris-Sud, 91405 Orsay, France
[2] Equipe mixte CEA-CNRS-UJF Nanophysique et Semiconducteurs, DRFMC/SP2M/PSC, CEA-Grenoble, 17 rue des Martyrs, 38054 Grenoble cedex 9, France

Received 30 September 2006, revised 23 November 2006, accepted 27 November 2006
Published online 16 May 2007

PACS 42.72.Ai, 73.21.Fg, 73.63.Hs, 78.30.Fs, 81.15.Hi, 85.60.Jb

This paper reports on GaN/AlN light-emitting devices relying on intersubband transitions. All samples have been grown by molecular beam epitaxy. We first present a systematic investigation of single or coupled GaN/AlN quantum wells grown by MBE. We then present the recent observation of strong ISB resonant enhancement of the second-harmonic generation of 1μm radiation. We finally report on the first observation of ISB luminescence in GaN QWs, which opens new prospects for the realization of nitride unipolar lasers based on current injection or optical pumping.

1 Introduction

Semiconductor materials can be made optically active at wavelengths irrespective of their band gap by engineering the electron quantum confinement in thin quantum well layers (QW). Quantum cascade lasers (QC) [1], quantum fountain lasers (QF) [2], quantum well infrared photodetectors (QWIP) [3] or modulators [4] are good illustrations of electron engineered devices. These control-by-design devices rely on optical intersubband (ISB) transitions between electron confined states and the desired wavelength of operation can be obtained through a proper choice of the layer thicknesses. Using standard ISB materials such as GaAs/AlGaAs, InGaAs/AlInAs or antimonides, the devices can be operated from the mid-infrared to the THz spectral range. Recently, wide-gap III-nitride semiconductors have attracted new attention because the large conduction band offset provided by their heterostructures offers the potential to push the ISB device operation to much shorter wavelengths, namely the 1.3–1.55 μm range used for fibre optics telecommunications.

Short-wavelength ISB absorptions have been reported by several groups in GaN/AlGaN QW samples grown by metal organic chemical vapor deposition (MOCVD) [5–7] or molecular beam epitaxy (MBE) [8–12]. Intraband absorption at telecommunication wavelengths has also been observed in self-organized GaN/AlN quantum dots [13–15]. Ultrathin GaN layers, typically 1–1.5 nm thick, are required to cover the 1.3–1.55 μm wavelength range [9, 12]. This is a consequence of the short target wavelength and of the rather large electron effective mass of GaN (3 times that of GaAs). Although rapid progress is being made in terms of MOVPE growth [16], MBE is still the most investigated technique for growing short-wavelength ISB devices because of its inherent slow growth rate, which allows accurate control of layer thicknesses down to one monolayer (1 ML = 0.2593 nm in relaxed GaN).

[*] Corresponding author: e-mail: francois.julien@ief.u-psud.fr, Phone: +33 1 69156299, Fax: +33 1 69154115

The ISB absorption recovery time of GaN/AlGaN QWs is extremely fast as a consequence of very efficient ISB scattering processes involving LO-phonons in these highly-polar materials [17–19]. It was measured to be in the range 150–400 fs. This key feature offers prospects for ultrafast ISB devices operating at Tbit/s data rates. Saturable ISB switches have been demonstrated [20, 21]. These ultrafast all-optical devices are of great interest for optical time division multiplexed systems. Applications to photodetection have also been investigated. GaN/AlN photodetectors based on either quantum well or quantum dot active regions have been demonstrated [22–25]. Electro-optical modulation devices operating at telecommunication wavelengths have also been recently reported [26].

In this paper, we focus on the recent progress towards light-emitting ISB devices [27, 28]. The building blocks for such devices are single or coupled GaN/AlN quantum well superlattices [12, 29]. We first present a systematic investigation of such structures grown by MBE. This study allows to get insight into the material parameters governing the electron quantum confinement at the ML scale. We then present the recent observation of strong ISB resonant enhancement of the second-harmonic generation of 1 μm radiation. We finally report on the first observation of ISB luminescence in GaN QWs, which opens new prospects for the realization of nitride unipolar lasers based on current injection or optical pumping.

2 GaN/AlN QW superlattice

We first present a systematic investigation of ISB transitions in ultrathin GaN/AlN QWs grown by plasma-assisted molecular-beam epitaxy (PAMBE) on *c*-sapphire substrates with an AlN buffer layer. The samples consist of 20 periods of GaN QWs with 3-nm-thick AlN barriers, sandwiched between two GaN claddings doped with silicon at a concentration of 1×10^{18} cm^{-3}. The thickness of the well ranges from 1 to 2.6 nm. The GaN wells are doped with Si at a concentration of 5×10^{19} cm^{-3}, while the AlN barriers are nominally undoped. The growth of the GaN wells and AlN barriers is performed at 720 °C using Ga as a surfactant [12]. Transmission electron microscopy (TEM) studies reveal chemically sharp AlN/GaN interfaces at the atomic layer scale.

The ISB absorption of the samples has been investigated at room temperature using a Fourier transform infrared spectrometer (FTIR). Two opposite facets of the sample have been polished at 45° angle to form a multi-pass waveguides with 4–6 total internal reflections. All samples show a pronounced p-polarized absorption peaked in the 1.33 to 1.91 μm wavelength range, which is ascribed to the e_1e_2 ISB absorption. Figure 1 displays the ISB absorbance spectra for samples with QW thickness varying from 1 to 1.5 nm. For such thin QWs the absorption covers the 1.3–1.55 μm wavelength range. Depending on

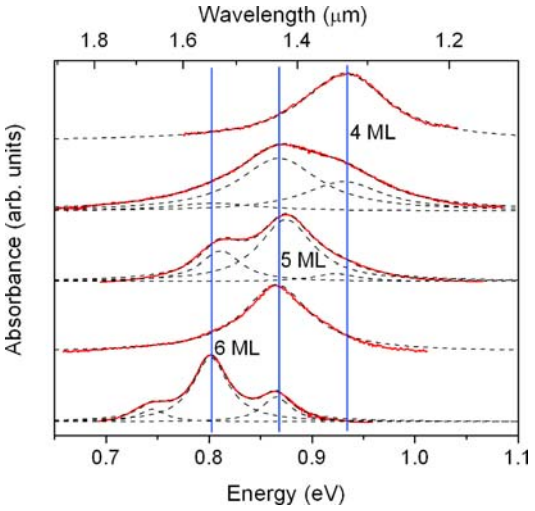

Fig. 1 (online colour at: www.pss-a.com) Absorbance spectra of multiple GaN/AlN QW samples (full lines) with corresponding Lorentzian fits (dashed lines), vertical lines mark the mean energies of the peaks.

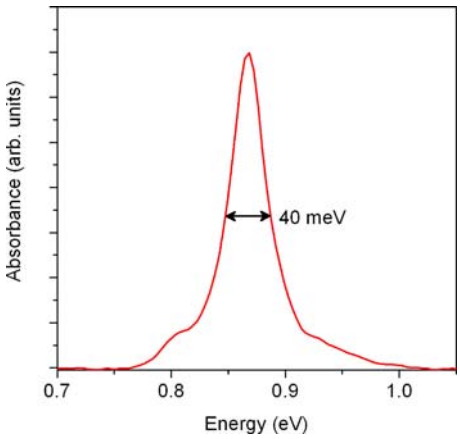

Fig. 2 (online colour at: www.pss-a.com) Room-temperature absorbance spectrum of a 20 period GaN/AlN superlattice with 3 nm thick AlN barrier and 1.3 nm thick GaN wells. The sample is nominally undoped. The ground state electron population of the wells is estimated to be $\approx 1 \times 10^{12}$ cm^{-2}.

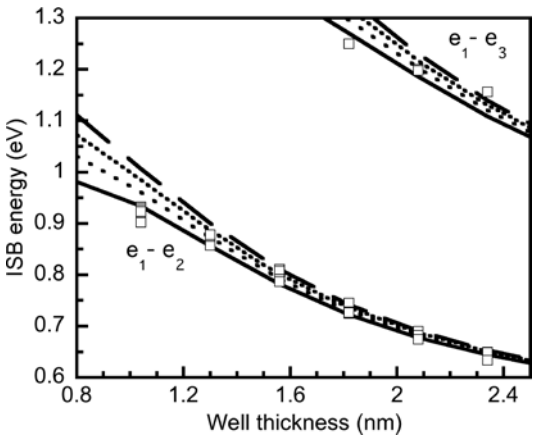

Fig. 3 ISB energy versus well thickness. The open squares are the experimental values. The curves are calculations assuming a conduction band offset of 1.95, 1.85, 1.75 and 1.65 eV from top to bottom, respectively. The polarization discontinuity at the GaN/AlN interfaces is taken as $\Delta P/\varepsilon\varepsilon_0 = 10$ MV/cm [12].

samples, the ISB spectrum shows either one peak or multiple peaks. The energy of the peaks coincides for the various samples. Each peak corresponds to the ISB absorption of GaN wells with a thickness equal to an integer number of monolayers, as discussed in detail in Ref. [12]. For all samples, the absorption line shape is perfectly fitted using either a single or multiple Lorentzian resonances. The Lorentzian line shape is a signature of homogeneously broadened transitions. The full width at half maximum (FWHM) of the single peak resonances is of the order of 65 meV, which corresponds to an electron dephasing time of 20 fs, in good agreement with reported values of the electron–electron scattering time [5]. Separate experiments performed on non-intentionally doped samples, where electron concentration is provided through residual doping, reveal even smaller broadening. Figure 2 shows the absorption spectrum of such a sample with a FWHM of 40 meV, which value sets a new state-of-the-art for ISB samples grown by MBE.

For QWs with a well thickness above 7 MLs, a weak p-polarized absorption is observed at high energy in addition to the main e_1e_2 absorption. We attribute the high-energy absorption to the transition from the ground subband e_1 to the third subband e_3 in agreement with previous observations by Hoshino et al. [30]. This transition, which is forbidden in a symmetric potential, is allowed in nitride QWs grown along the polar *c*-axis because of the presence of the strong internal electric field in the well, which breaks the symmetry of the potential.

The electron quantum confinement was modeled within the envelope function approximation taking into account the conduction band non-parabolicity by means of an energy-dependent effective mass. The doping-related effects are included via the self-consistent solution of the Schrödinger–Poisson equations with the subsequent application of the many-body corrections. A detailed description of the model and of the used parameters can be found in Ref. [12]. The model predicts a blue-shift of the ISB absorption energy with increasing electron concentration in the wells as a result of many-body effects dominated by the exchange interaction, in agreement with experiments [11]. As shown in Fig. 3, the best agreement with measurements of the ISB transition energy versus well thickness is achieved for a conduction band offset of 1.7 ± 0.05 eV, which value is significantly smaller than the previously admitted value of 2 eV.

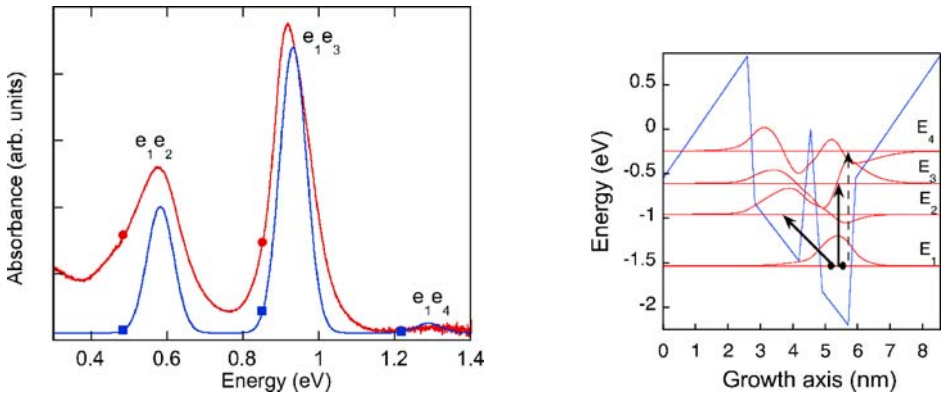

Fig. 4 (online colour at: www.pss-a.com) Left – Measured (circles) and calculated (squares) absorbance spectrum of the GaN/AlN CQW sample with 2 ML AlN coupling barrier. Right – CB profile and the corresponding electronic levels of the CQWs assuming a potential drop spread over 1 ML at the interfaces. Arrows mark the observed ISB transitions.

3 Coupled GaN/AlN QWs

Many ISB devices such as electro-optical modulators, quantum cascade or quantum fountain lasers require active structures beyond the single QW. The study of coupled quantum wells (CQW) is therefore a key point for the development of these optoelectronic components in nitrides. Because of the large potential discontinuity at the GaN/AlN interface, ultrathin (0.5–1 nm) AlN barriers are required to achieve effective electron coupling between the wells. We have investigated samples grown by PAMBE on AlN/*c*-sapphire templates containing 20 periods of double QWs separated by 3 nm thick AlN spacer layers. The double QWs consist of 3–7 ML thick GaN wells coupled with a 1–2 ML thick AlN barrier. The second QW with respect to the growth direction is doped with silicon at 5×10^{19} cm^{-3} in order to populate the ground electronic state. TEM measurements reveal sharp interfaces as well as a control of the layer thicknesses down to 1 ML [29].

Figure 4 shows the absorbance of a CQW sample with a 2 ML thick coupling barrier for p-polarized light. The sample exhibits two pronounced absorptions peaked at 0.58 eV (2.14 μm) and 0.926 eV (1.34 μm) in addition to a weak absorption at 1.3 eV (0.95 μm). No absorption is observed for s-polarized light within experimental accuracy. The absorptions at 0.58, 0.926 and 1.3 eV are ascribed to the ISB transitions e_1e_2, e_1e_3 and e_1e_4, respectively. It should be noted that the observation of the e_1e_2 transition between the ground states of the two wells is a signature of the strong electronic coupling by the ultrathin AlN barrier. The FWHM of the ISB absorptions is in the range of 130–160 meV, which is significantly larger than the state-of-the-art value of 40 meV measured for single QWs. The larger broadening for the CQWs can be explained by the delocalization of the excited electrons between the two QWs. Indeed, in this case the ISB energy becomes very sensitive to thickness or internal field fluctuations in the GaN wells and AlN coupling barrier.

We have simulated the CQWs using the model described above. No satisfactory agreement with observations could be obtained assuming an abrupt potential drop at the GaN/AlN interfaces. In contrast, as shown in Fig. 4, the agreement is excellent in terms of ISB energies and oscillator strengths when considering that the potential drop at the GaN/AlN heterointerfaces is spread over 1 ML (the resulting CB profile is shown in Fig. 4 right) [29, 31].

4 ISB light generation through second-order optical nonlinearities

The second-order non-linear susceptibility is known to be strongly enhanced in semiconductor QWs when the waves are in close resonance with ISB transitions [32]. However, an asymmetric potential is

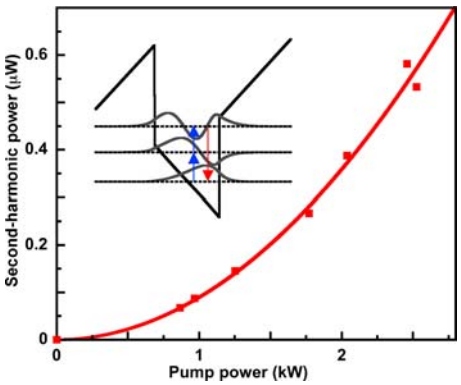

Fig. 5 (online colour at: www.pss-a.com) Second harmonic power versus pump power (full squares) and quadratic fit (solid curve). The inset shows the conduction band profile of the 10 ML thick GaN/AlN QWs.

required to benefit from the ISB resonance enhancement since the second-order nonlinear susceptibility is identically zero in a potential with inversion symmetry. Resonant second harmonic generation (SHG) in the mid-infrared spectral range has been reported in various material systems such as GaAs/AlGaAs, AlInAs/GaInAs or SiGe/Si [33]. The asymmetric potentials were provided either by bias application, step-like composition or asymmetric coupled QWs. In contrast to these materials, hexagonal-phase GaN/AlGaN QWs grown along the *c*-axis naturally exhibit an asymmetric saw-tooth potential, which arises from the piezo-electric and spontaneous polarization discontinuity between the well and barrier materials. In addition, because of the large band offset, ISB resonant enhancement of SHG in GaN/AlN QWs can be expected at much shorter infrared wavelengths.

A test sample was grown by PAMBE on an AlN/*c*-sapphire template. The active region contains 200 periods of nominally 10 ML thick GaN wells separated by 3 nm thick AlN spacer layers. The sample is non-intentionally doped. The electron concentration in the ground subband is measured to be 1.05×10^{12} cm^{-2}. ISB spectroscopy reveals a strong e_1e_2 absorption peak at 1.95 μm wavelength (FWHM 84 meV) as well as a weak e_1e_3 absorption at 1.05 μm wavelength.

The SHG measurements have been performed at room temperature using optical pumping by a pulsed optical parametric oscillator tunable in the wavelength range of 1.9–2.1 μm. The output beam was focused onto the sample orientated at Brewster's angle. Figure 5 shows the power emitted at ~1 μm wavelength versus the peak pump power. The pump wavelength is 1.98 μm and the pump beam is p-polarized. The emitted power closely follows a quadratic law with pump power, as expected for a SHG process. In addition, the signal vanishes either when the pump beam is s-polarized or when the sample is rotated at normal incidence, as expected from ISB polarization selection rules. Separate experiments performed on an AlN/*c*-sapphire template reference sample do not show any measurable signal within our detection limit. This confirms that the signal generated in the QW sample arises from the GaN wells and not from the AlN buffer layer.

Figure 6 shows a plot of the square modulo of the second-harmonic susceptibility versus the pump photon energy for the QW sample in addition to the absorption spectrum at Brewster's angle of incidence. As seen in Fig. 6, the second-harmonic signal exhibits a strongly resonant behavior. The conversion efficiency is peaked at 2.0 μm wavelength. The FWHM of the resonant peak is 18 meV, which corresponds to a reduction by a factor 2.33 of the linewidth with respect to the ISB absorption of the 10 ML thick QW. This value of the linewidth reduction is very close to the theoretical value, 2.39 predicted for a second-harmonic process relying on double-resonance enhancement [34]. Separate experiments performed on a sample containing a bulk GaN buffer layer grown on *c*-sapphire do not show any resonant enhancement in the investigated pump wavelength range.

The conversion at a pump wavelength of 2.0 μm is found to be 16 times more efficient in the QW sample with respect to a bulk GaN reference sample of similar thickness. The value of the second-order nonlinear susceptibility $\chi^{(2)}_{zzz}$ is deduced to be 114 pm/V for the QW sample and 28 pm/V for the GaN reference sample. The second-order nonlinear susceptibility of the GaN QWs is 4 times larger than that

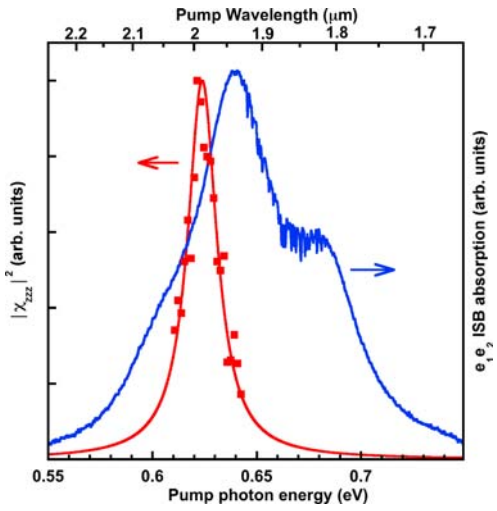

Fig. 6 (online colour at: www.pss-a.com) Left scale: squared modulo of the second harmonic susceptibility versus pump photon energy (full squares are measurements, solid curve is a Lorentzian fit). Right scale: absorption spectrum at Brewster's angle of incidence. The peak at 1.95 μm (1.82 μm) is the e_1e_2 ISB absorption of GaN/AlN QWs with a well thickness of 10 (9) ML.

of bulk GaN and 2 times larger than that of $LiNbO_3$. It should be noted that $\chi^{(2)}_{zzz}$ is proportional to the carrier concentration in the well, which is only provided by residual doping in the present sample. Stronger resonant enhancement and larger second-order nonlinear susceptibility can be expected in Si doped GaN QWs.

5 Room-temperature ISB luminescence from GaN/AlN QWs

It is well known that the ISB luminescence is a very inefficient process because of the very short non-radiative electron-LO phonon scattering times. This translates into an extremely low ISB luminescence efficiency. Such a low value makes the detection of spontaneous emission very challenging. This weak luminescence efficiency is a characteristic of all ISB emitters. It does not prevent the realization of high performance unipolar lasers [1, 2]. In the lasing regime, the stimulated emission rate becomes very large thanks to the strong oscillator strength associated with ISB transitions.

We have investigated the ISB luminescence of GaN/AlN QWs designed to exhibit three bound states in the conduction band. It contains 250 periods of 2 nm thick GaN QW layers separated by 3 nm thick AlN barriers grown by PAMBE on a 1 μm thick AlN buffer on *c*-sapphire. The wells are doped

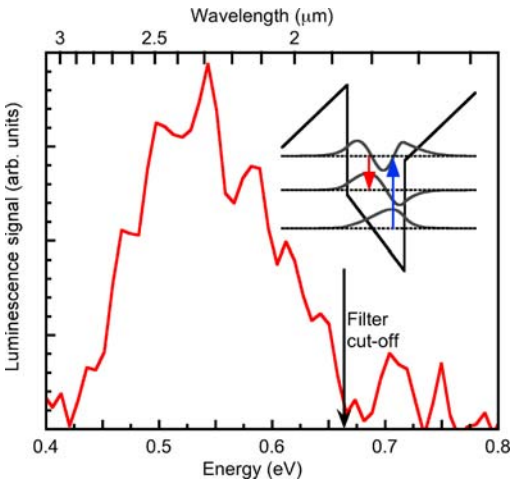

Fig. 7 (online colour at: www.pss-a.com) Room-temperature ISB emission spectrum under resonant excitation of the e_1-e_3 ISB transition. The spectral response of the optics and detector is flat at wavelengths between 2 and 2.9 μm. The inset shows the conduction band profile of an 8 ML thick GaN/AlN QW.

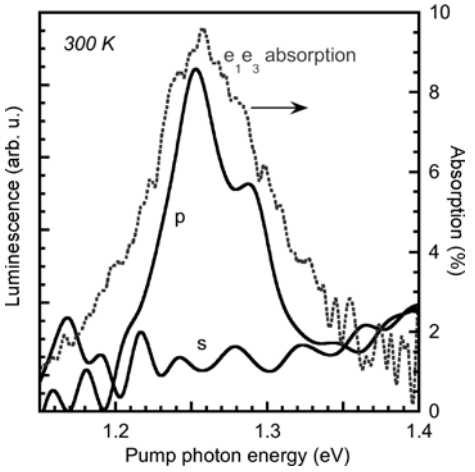

Fig. 8 Left scale: luminescence signal versus pump photon energy under p- or s-polarized excitation. Right scale: e_1e_3 ISB absorption spectrum (dotted curve).

with silicon at a concentration of 5×10^{19} cm^{-3}. The e_1e_2 and e_1-e_3 ISB absorptions are observed at $\lambda = 1.67$ μm and $\lambda = 0.98$ μm, respectively.

The emission measurements have been performed at room temperature using resonant optical pumping at the e_1-e_3 ISB transition energy. The optical excitation is provided by a tunable Ti:sapphire near-infrared laser operated in continuous wave. The pump beam is focused onto the sample facet polished at 45° angle. The emission from the opposite facet of the sample is collected with a spherical mirror and directed onto the emission port of the FTIR spectrometer operated in step-scan mode. A 5 mm thick Ge plate is used to reject the residual pump light. Detection is performed with a liquid nitrogen cooled InAs detector.

Figure 7 shows the emission spectrum of the sample under p-polarized excitation at $\lambda \sim 0.98$ μm in resonance with the e_1-e_3 transition. The pump power is 1 W. As seen in Fig. 7, the emission is peaked at $\lambda = 2.3$ μm (0.54 eV) with a FWHM of 160 meV. The peak position is very close to the expected energy (0.535 eV) of the e_3-e_2 ISB transition deduced from transmission measurements. The emission is mainly p-polarized, as expected from ISB polarization selection rules, with a ratio between p- and s-polarization exceeding a factor of 3. The residual s-polarized signal is probably due to depolarization effects because of multiple reflections inside the sample. As shown in Fig. 8, the emission signal vanishes when the pump beam polarization is rotated from p (TM) to s (TE)-polarization. This is a proof that the luminescence originates from ISB transitions in the QWs. Another signature of the ISB origin of the signal is obtained by tuning the pump laser wavelength. As seen in Fig. 8, the luminescence signal closely follows the e_1-e_3 absorption lineshape. The efficiency of the collected e_3-e_2 ISB luminescence is measured to be in the range 10 pW per Watt of pump power.

6 Conclusions

We have reported a thorough investigation of the ISB absorption and emission properties of GaN/AlN heterostructures grown by PAMBE. Both single and coupled quantum wells have been investigated experimentally and theoretically. Large second-order nonlinearities at $\lambda = 1$ μm due to ISB resonant enhancement have been demonstrated. This study opens new prospects for the development of efficient nonlinear devices relying on quasi phase-matching techniques. Finally, the ISB luminescence from GaN/AlN QWs at room temperature is demonstrated. This result represents the first step towards the realization of optically pumped QF lasers and amplifiers operating at telecommunication wavelengths. Nitride-based QC lasers are also of great interest. However, these devices raise numerous challenges in terms of epitaxial growth and control of vertical transport of electrons.

Acknowledgements The authors wish to acknowledge T. Remmele, M. Albrecht, E. Bellet-Almaric, M. Raybaut, A. Godard, and E. Rosencher for fruitful collaboration. This work was supported by European FP6 NitWave program (contract IST #04170).

References

[1] J. Faist, F. Capasso, D. Sivco, C. Sirtori, A. L. Hutchinson, S. N. G. Chu, and A. Y. Cho, Science **264**, 553 (1994).
[2] O. Gauthier-Lafaye, P. Boucaud, F. H. Julien, S. Sauvage, S. Cabaret, J. M. Lourtioz, V. Thierry Mieg, and R. Planel, Appl. Phys. Lett. **71**, 3619 (1997).
O. Gauthier-Lafaye, B. Seguin-Roa, F. H. Julien, P. Collot, C. Sirtori, J. Y. Duboz, and G. Strasser, Physica E **7**, 12 (2000).
[3] B. F. Levine, K. K. Choi, C. G. Bethea, J. Walker, and R. J. Malik, Appl. Phys. Lett. **50**, 1092 (1987).
[4] F. H. Julien, P. Vagos, J.-M. Lourtioz, D. D. Yang, and R. Planel, Appl. Phys. Lett. **59**, 2645 (1991).
[5] N. Suzuki and N. Iizuka, Jpn. J. Appl. Phys. **36**, L1006 (1997).
[6] I. Waki, C. Kumtornkittikul, Y. Shimogaki, and Y. Nakano, Appl. Phys. Lett. **82**, 4465 (2003); Appl. Phys. Lett. **84**, 3703 (2004).
[7] S. Nicolay, J.-F. Carlin, E. Feltin, R. Butté, M. Mosca, N. Grandjean, M. Ilegems, M. Tchernycheva, L. Nevou, and F. H. Julien, Appl. Phys. Lett. **87**, 111106 (2005).
[8] C. Gmachl, H. M. Ng, S. N. G. Chu, and A. Y. Cho, Appl. Phys. Lett. **77**, 3722 (2000).
C. Gmachl, H. M. Ng, and A. Y. Cho, Appl. Phys. Lett. **79**, 1590 (2001).
[9] K. Kishino, A. Kikuchi, H. Kanazava, and T. Tachibana, Appl. Phys. Lett. **81**, 1234 (2002).
[10] N. Iizuka, K. Kaneko, and N. Suzuki, Appl. Phys. Lett. **81**, 1803 (2002).
[11] A. Helman, M. Tchernycheva, A. Lusson, E. Warde, F. H. Julien, Kh. Moumanis, G. Fishman, E. Monroy, B. Daudin, D. Le Si Dang, E. Bellet-Amalric, and D. Jalabert, Appl. Phys. Lett. **83**, 5196 (2003).
[12] M. Tchernycheva, L. Nevou, L. Doyennette, F. H. Julien, E. Warde, F. Guillot, E. Monroy, E. Bellet-Amalric, T. Remmele, and M. Albrecht, Phys. Rev. B **73**, 125347 (2006).
[13] K. Moumanis, A. Helman, F. Fossard, M. Tchernycheva, A. Lusson, F. H. Julien, B. Damilano, N. Grandjean, and J. Massies, Appl. Phys. Lett. **82**, 868 (2003).
[14] M. Tchernycheva, L. Nevou, L. Doyennette, A. Helman, R. Colombelli, F. H. Julien, F. Guillot, E. Monroy, T. Shibata, and M. Tanaka, Appl. Phys. Lett. **87**, 101912 (2005).
[15] F. Guillot, E. Bellet-Amalric, E. Monroy, M. Tchernycheva, L. Nevou, L. Doyennette, F. H. Julien, Le Si Dang, T. Remmele, M. Albrecht, T. Shibata, and M. Tanaka, Appl. Phys. **100**, 044326 (2006).
[16] E. Baumann, F. R. Giorgetta, D. Hofstetter, S. Golka, W. Schrenk, G. Strasser, L. Kirste, S. Nicolay, E. Feltin, J. F. Carlin, and N. Grandjean, Appl. Phys. Lett. **89**, 041106 (2006).
[17] N. Iizuka, K. Kaneko, N. Suzuki, T. Asano, S. Noda, and O. Wada, Appl. Phys. Lett. **77**, 648 (2000).
[18] J. D. Heber, C. Gmachl, H. M. Ng, and A. Y. Cho, Appl. Phys. Lett. **81**, 1237 (2002).
[19] J. Hamazaki, S. Matsui, H. Kunugita, K. Ema, H. Kanazawa, T. Tachibana, A. Kikuchi, and K. Kishino, Appl. Phys. Lett. **84**, 1102 (2004).
[20] N. Iizuka, K. Kaneko, and N. Suzuki, J. Appl. Phys. **99**, 093107 (2006).
[21] N. Iizuka, K. Kaneko, and N. Suzuki, IEEE J. Quantum Electron. **42**, 765 (2006).
[22] D. Hofstetter, S. Schad, H. Wu, W. J. Schaff, and L. F. Eastman, Appl. Phys. Lett. **83**, 572 (2003).
[23] D. Hofstetter, E. Baumann, F. R. Giorgetta, M. Graf, M. Maier, F. Guillot, E. Bellet-Amalric, and E. Monroy, Appl. Phys. Lett. **88**, 121112 (2006).
[24] L. Doyennette, L. Nevou, M. Tchernycheva, A. Lupu, F. Guillot, E. Monroy, R. Colombelli, and F. H. Julien, Electron. Lett. **41**, 1077 (2005).
[25] A. Vardi, N. Akopian, G. Bahir, L. Doyennette, M. Tchernycheva, L. Nevou, F. H. Julien, F. Guillot, and E. Monroy, Appl. Phys. Lett. **88**, 143101 (2006).
[26] E. Baumann, F. R. Giorgetta, D. Hofstetter, S. Leconte, F. Guillot, E. Bellet-Amalric, and E. Monroy, Appl. Phys. Lett. **89**, 101121 (2006).
[27] L. Nevou, M. Tchernycheva, F. Julien, M. Raybaut, A. Godard, E. Rosencher, F. Guillot, and E. Monroy, Appl. Phys. Lett. **89**, 151101 (2006).
[28] L. Nevou, F. Julien, R. Colombelli, F. Guillot, and E. Monroy, Electron. Lett. **42**, 1308 (2006).
L. Nevou, M. Tchernycheva, F. H. Julien, F. Guillot, and E. Manroy, Appl. Phys. Lett. **90**, 121106 (2007).

[29] M. Tchernycheva, L. Nevou, L. Doyennette, F. H. Julien, F. Guillot, E. Monroy, T. Remmele, and M. Albrecht, Appl. Phys. Lett. **88**, 153113 (2006).
[30] K. Hoshino, T. Someya, K. Hirakawa, and Y. Arakawa, phys. stat. sol. (a) **192**, 27 (2003).
[31] F. Bernardini and V. Fiorentini, Phys. Rev. B **57**, R9427 (1998).
[32] M. K. Gurnick and T. A. DeTemple, IEEE J. Quantum Electron. **QE-19**, 791 (1983).
[33] M. M. Fejer, S. J. B. Yoo, R. L. Byer, A. Harwit, and S. J. Harris, Jr., Phys. Rev. Lett. **62**, 1041 (1989).
[34] E. Rosencher and P. Bois, Phys. Rev. B **44**, 11315 (1991).